Smoothness Implies Determinism: A Method to Detect It in Time Series

Liming W. Salvino and Robert Cawley
Naval Surface Warfare Center, Dahlgren Division, Silver Spring, Maryland 20903-5640
(Received 27 May 1993)

Continuity on an embedded phase space is enough to imply determinism in time series. Also, it is possible to define infinitely many arbitrary vector fields over an attractor. We exploit this arbitrariness to generate a detector of smoothness and therefore of determinism in time series. We report results of numerical studies of both flow and map examples and of a chaotic experimental system.

PACS numbers: 05.45.+b

The advent of chaos, which is deterministic, has led to a new desire among researchers to detect determinism in time series. One catalyst for this is surely the simple geometric picture of the phase portrait of a dynamical system behaving chaotically, and the possibility of realizing it from observed scalar time series with simple embedding methods [1,2]. Recently there have been some new approaches to the problem [3–6] that are more direct than older efforts based on attempting to estimate data observables physically meaningful for the context of determinism. These include fractal dimensions, Lyapunov exponents, and other geometrical and dynamical quantities. A feature of the method we describe herein, distinguishing it from previous ones, is the existence of a theorem *guaranteeing* determinism if a simple test is met. Our approach has been presaged by [4] and [6].

It is actually a fact that smoothness in phase space implies determinism in time series. We describe a test for detecting that smoothness, and thus determinism. In addition, we have devised a novel surrogate comparison test to distinguish smoothness from nonsmooth behavior for chosen types of randomness. In both cases we can largely remove ambiguities from dependence on delay caused by finite numerics. This is done through a unique theoretical device [Eq. (2)] which exploits smoothness of the phase portraits to define an infinite class of vector fields for any system.

The mathematical situation is this: Chaotic behavior is produced by nonlinear ordinary differential equations and maps on manifolds. As long as the right hand side of a system of ordinary differential equations is a smooth (i.e., locally Lipshitz) function of position, its solutions are uniquely fixed from any given initial condition, and nearby points on the phase space behave similarly under time evolution. These continuity properties thus imply unique future behavior; that is, *smoothness implies determinism* [7].

Maps are slightly different. Here the issue is not one of uniqueness of solutions; if the map is specified, the nth iterate is determined, even if the map is not continuous. But the establishment of smoothness means there actually *is* a rule that can be determined for the evolution of points, that provided by the data on the embedded space.

Our method is simple and easy to implement. Let an observed time series, $v(t)$: $t = 1,\ldots,N_D$, be the output of a differentiable dynamical system f^t on an m-dimensional manifold M; i.e., f^t: $M \to M$, where f^t is the tth iterate of f, is the nonlinear dynamics underlying the data, and $v(t)$ is the measured time history of one of the coordinates for the orbit in M. When the delays are introduced an embedding of M into $\mathbb{R}^d$ typically results as long as the number of components, d, is made large enough [2]. Smoothness properties of the dynamical system are now reproduced in the embedded image of M in $\mathbb{R}^d$. The delay vector time series, $x(t) = (v(t), v(t+\Delta),\ldots, v(t+(d-1)\Delta))$, where Δ is the delay, and $t = 1,\ldots,N = N_D - (d-1)\Delta$, lives in that image. Its behavior carries the smoothness.

We denote the time-one map, i.e., f^1, by F and consider the following general quantity:

$$\phi = \phi(x) = \Psi(x, F^b(x),\ldots,F^{b(R-1)}(x)), \qquad R > 1, \tag{1}$$

where F^b denotes the bth iterate of F and where Ψ is some smooth function of its R vector arguments into $\mathbb{R}^d$. $\phi(x)$ is a vector field in $\mathbb{R}^d$; i.e., the vector ϕ is (merely) a function of the position x. We take $b = 1$ here for simplicity. A simple form for $\phi(x)$ is

$$\phi(x) = \sum_{r=0}^{R-1} c_r F^r(x), \qquad R > 1. \tag{2}$$

F may be an arbitrarily sampled flow, or a map; $F^0(x(t)) = x(t)$, $F^1(x(t)) = x(t+1)$, etc. The c_r are at our disposal, and we now take them to be constants, independent of x.

Directional (unit vector) fields for $\phi(x)$ for dynamical systems are smooth and depend on the choice of the c_r. To estimate such fields we partition the phase space by a uniform grid. We call the jth mesh cell of points, comprised of the x_i, $i = 1,\ldots,n_j$, box j, and we compute the average of the directional elements, $\hat{x} = \phi(x)\,\|\phi(x)\|^{-1}$, over box j,

$$Y_j = n_j^{-1} \sum_{i=1}^{n_j} \hat{x}(x_i). \tag{3}$$

0031-9007/94/73(8)/1091(4)$06.00

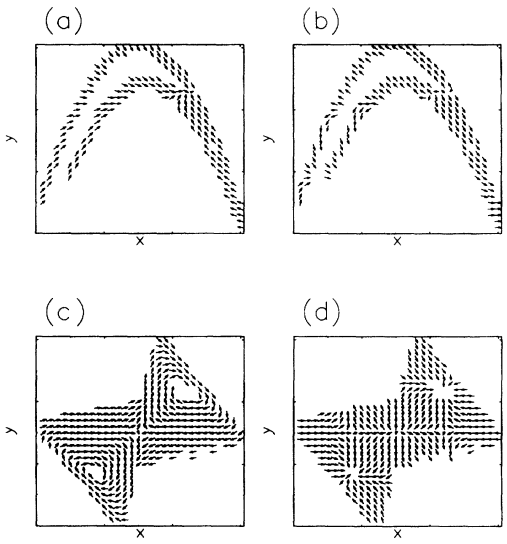

FIG. 1. Directional element fields for $d = 2$ for Hénon map (delay $\Delta = 1$) and Lorenz system ($\Delta = 4$). Data length $N = 20\,000$, grid size $n^2 = 30 \times 30$. (a) Hénon: $\{c_r\} = \{-1, 1\}$. (b) Hénon: $\{c_r\} = \{2, -5, 3\}$. (c) Lorenz: $\{c_r\} = \{-1, 1\}$. (d) Lorenz: $\{c_r\} = \{2, -5, 3\}$.

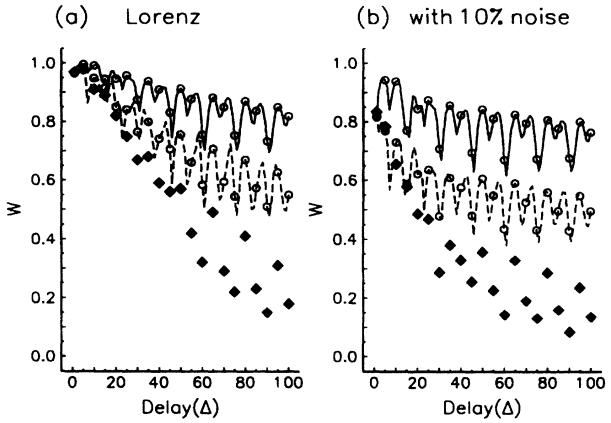

FIG. 2. Vector field dependence of computed values of W. $\{c_r\} =: \{1, 2, 3, -4, -2\}$ (solid curve), $\{-1, 1\}$ (dashed curve). Also shown is a comparison with Λ statistic of [4] (solid diamonds).

We compute Y_j for Lorenz system [$\dot{x} = 10(y - x)$, $\dot{y} = 28x - y - xz$, $\dot{z} = -\frac{8}{3}z + xy$, sampling time $\Delta t = 0.05$ (17 points/cycle)] and Hénon map ($x' = 1 - 1.4x^2 + y$, $y' = 0.3x$) data for illustration (Fig. 1). The vector time series were computed from the delay coordinate construction on the x coordinate for each case. We note the choice $\{c_r\} = \{-1, 1\}$ produces a directional field whose "arrows" point to the position of the next iterate. For finely sampled flows this vector field approximates the flow line tangent vector field.

A measurement on a phase portrait that is independent of the choice of vector field when the time series is deterministic is easily formed from a global average of a mean local directional element length estimate based on Eq. (3); e.g., proceeding in the spirit of [4],

$$W = N^{-1} \sum_j n_j \|Y_j\|^2 . \tag{4}$$

Practically any function of the $\|Y_j\|$ can serve; Eq. (4) is just a weighted mean square.

For smooth data, $\|Y_j\| = 1$ for box j sufficiently small, and $W = 1$ should result. In fact, owing to finite numerics, W is often a lot less than 1. In particular, W depends on embedding parameters; for fixed d, $W = W(\Delta)$. W also depends on the choice of vector field ϕ. And the "natural" choice $\{c_r\} = \{-1, 1\}$, implicit in the methods of Refs. [4,6], does not necessarily produce the most deterministic looking $W(\Delta)$ (Fig. 2). We observe that corresponding numerical data for the Λ statistic of Ref. [4] lie a little below the lower curves. Also, the poorer performance of the $\{-1, 1\}$ vector field was not an isolated example, but, in fact, was common. Computation parameters for the study in Fig. 2 were $d = 3$, $N_D = 20\,000$ and the grid size, set by maximum range of the data, was $n^3 = 40 \times 40 \times 40$. Except where stated, we use these values henceforth.

Since $W = 1$ is supposed to hold for any $\{c_r\}$, the choice of vector field is arbitrary. This gives us a tool to deal with the finite numerics problem just noted, for now we can exploit the very wide range of options available from Eq. (3). We choose ten vector fields (Table I) and identify maximum values of W for each delay Δ. We display the maxima in plots against Δ (Fig. 3). As Δ rises the upper envelope of the $W(\Delta)$ descends to a well-defined minimum, $W_M \simeq 1$, viz., $0.9 < W_M < 1.0$. We note here the need to set a determinism tolerance limit for $W_M \simeq 1$, which we have taken to be 0.9. The largest delays in Fig. 3 correspond to about 180 cycles for the Lorenz and Rössler systems. We also did the computations for $N_D = 3000$, on a coarser grid, $n^3 = 30 \times 30 \times 30$, and for $N_D = 500$, grid size, $n^3 = 20 \times 20 \times 20$. W

TABLE I. Coefficients c_r for ten vector fields ϕ_n, $n = 1, \ldots, 10$, used in computations of $\Lambda(\Delta)$.

	c_0	c_1	c_2	c_3	c_4
ϕ_1	−1.0	1.0	0.0	0.0	0.0
ϕ_2	−3.0	4.0	−1.0	0.0	0.0
ϕ_3	2.0	−5.0	3.0	0.0	0.0
ϕ_4	4.7	−3.0	−1.7	0.0	0.0
ϕ_5	−2.0	3.0	−4.0	3.0	0.0
ϕ_6	3.5	−2.7	−1.4	0.6	0.0
ϕ_7	−3.4	−0.5	−0.1	4.0	0.0
ϕ_8	1.0	2.0	3.0	−4.0	−2.0
ϕ_9	0.9	0.8	−3.5	4.0	−2.2
ϕ_{10}	3.0	−2.0	0.0	2.0	−3.0

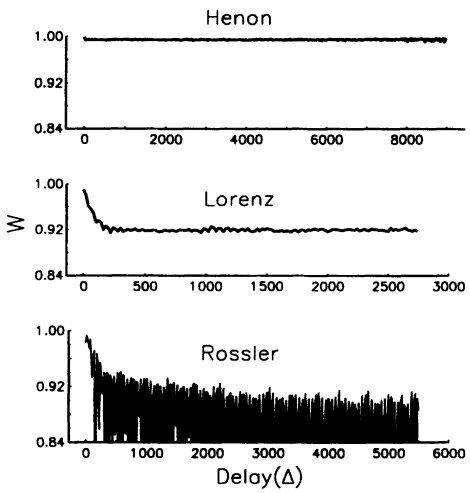

FIG. 3. Determinism case studies for three familiar chaotic systems. Computed W values shown are maxima for each delay over ten arbitrarily chosen vector fields.

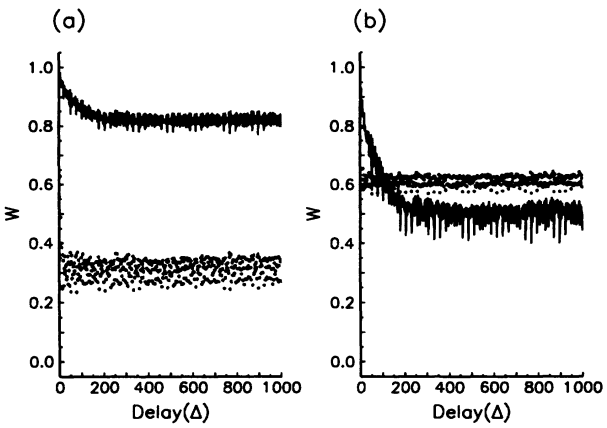

FIG. 4. $W(\Delta)$ plots for comparison test analysis of ribbon data: solid, given data; coded, randomized surrogate data. For each Δ, W is (a) maximum for data, minimum for surrogate; (b) minimum for data, maximum for surrogate.

plots were flatter, but their general features were similar; W_M values out to $\Delta = 1000$ and $\Delta = 200$, respectively, were all just as high. For the Rössler time series we used the x-coordinate solution to $\dot{x} = -(y + z)$, $\dot{y} = x + 0.2y$, $\dot{z} = 0.2 + zx - 5.7z$, sampling time $\Delta t = 0.2$ (30 points/cycle).

But maximum W plots for deterministic data also can yield estimates somewhat less than $W_M \simeq 1.0$, e.g., $0.7 < W_M < 0.9$; we represent this very crudely by writing $W_M \sim 1.0$. This happened with an experimental time series known to be chaotic. The upper W plot in Fig. 4(a) is the same quantity we computed for the studies in Fig. 3, but now the time series (14 points/cycle) represents the horizontal displacement of the base of the magnetostrictive ribbon in the experiment of Ref. [8]. From the figure, $W_M = 0.85$.

Here a simple comparison test can distinguish the given data as deterministic as opposed to random. We make use of surrogate time series, which may be specified in any of a number of ways [9]; and we use again the arbitrariness in the choice of vector field.

We generated surrogate data from the Fourier transform (periodogram) of the given data by randomizing the phases and transforming back. We then computed minimum $W(\Delta)$ values as well as maximum for both surrogate and given data. Organizing the results as shown in Fig. 4, we easily distinguish the given data from such a random surrogate. For suppose the data had been some other realization of the surrogate. Panels (a) and (b) would look exactly alike. This happened when we examined ambient ocean acoustic sonobuoy data (Fig. 5). Thus the acoustic plots show little evidence of determinism, while the ribbon data show strong evidence of determinism.

In cases like this we *should* go further, in particular by testing for additional classes of surrogate, but also by testing noise reduced versions of the given time series. We did the latter for the ribbon data, finding $W_M = 0.91$ [10]. Thus we have gained an absolute call for the ribbon system time series (i.e., $W_M \simeq 1$). We note the absolute call should be understood as relative to the determinism tolerance limit mentioned earlier. Obviously, we might not always be able to accomplish an absolute call, and the surrogate comparison test can provide a valuable fallback position for cases where determinism is yet likely.

We have presented a test to detect smoothness in phase space, which implies determinism in a given time series, i.e., $W_M \simeq 1.0$. Ambiguities from dependence on delay due to finite numerics are substantially mitigated through a novel theoretical device, of the use of many vector fields. Thus upper envelope values of maximum W plots now can be sensibly constant out to very high delay; or, if they fall away, they still level off to well-defined minima, again out to very high delay. We have

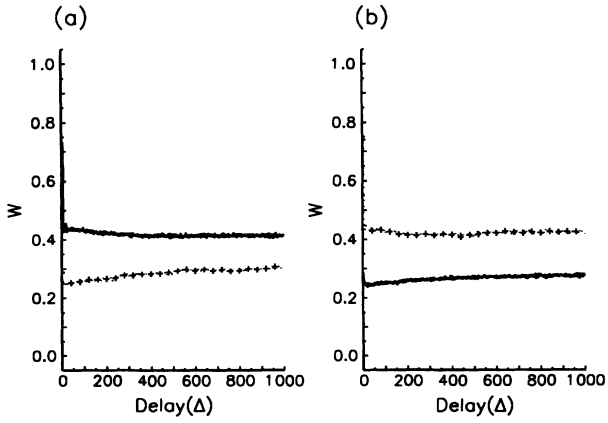

FIG. 5. Same as Fig. 4, but for ambient ocean acoustic data.

found stable, high values of W_M for both short and long time series. For marginal or negative cases we have provided a surrogate comparison test which sometimes can discriminate between smoothness and any chosen surrogate randomness. We have reported applications to a variety of examples.

We wish to thank Jim Yorke and Celso Grebogi for helpful criticism regarding our presentation and W. L. Ditto for the ribbon data. L. W. S. wishes to thank Sarah Little for the use of her personal computing facilities and Danny Kaplan for permission to use his code. R. C. wishes to thank Guan-Hsong Hsu for discussions about smoothness and determinism. This work has been supported by the Office of Naval Research (Physics) and by the NSWCDD Independent Research Program.

[1] N. H. Packard, J. P. Crutchfield, J. D. Farmer, and R. S. Shaw, Phys. Rev. Lett. **45**, 712 (1980).

[2] F. Takens, in *Dynamical Systems and Turbulence, Warwick, 1990,* edited by D. A. Rand and L.-S. Young, Lecture Notes in Mathematics Vol. 898 (Springer-Verlag, Berlin, 1981), pp. 366–381.

[3] G. Sugihara and R. M. May, Nature (London) **344**, 734 (1990).

[4] D. T. Kaplan and L. Glass, Phys. Rev. Lett. **68**, 427 (1992); D. T. Kaplan and L. Glass, Physica (Amsterdam) **64D**, 431 (1993).

[5] M. B. Kennel and S. Isabelle, Phys. Rev. A **46**, 3111 (1992).

[6] R. Wayland, D. Bromley, D. Pickett, and A. Passamante, Phys. Rev. Lett. **70**, 580 (1993).

[7] A flow that is only C^0 need not evolve uniquely (deterministically) from a given initial condition. A simple one-dimensional example of a nondeterministic C^0 system is $\dot{x} = (1 - x^2)^{1/2}$, $x(0) = 0$.

[8] W. L. Ditto, S. N. Rauseo, R. Cawley, C. Grebogi, G.-H. Hsu, E. Kostelich, E. Ott, H. T. Savage, R. Segnan, M. L. Spano, and J. A. Yorke, Phys. Rev. Lett. **63**, 923 (1989).

[9] James Theiler, Stephen Eubank, André Longtin, Bryan Galdrikian, and J. Doyne Farmer, Physica (Amsterdam) **58D**, 77 (1992).

[10] We used the local geometric projection method of R. Cawley and G.-H. Hsu, Phys. Rev. A **46**, 3057 (1992).